6-1-2020

Differential expression of glucose transporters and hexokinases in prostate cancer with a neuroendocrine gene signature: A mechanistic perspective for 18 F-FDG imaging of PSMA-suppressed tumors

Martin K. Bakht
University of Windsor

Jessica M. Lovnicki
The University of British Columbia

Janice Tubman
University of Windsor

Keith F. Stringer
University of Windsor

Jonathan Chiaramonte
University of Windsor

Recommended Citation

See next page for additional authors
Bakht, Martin K.; Lovnicki, Jessica M.; Tubman, Janice; Stringer, Keith F.; Chiaramonte, Jonathan; Reynolds, Michael R.; Derecichei, Iulian; Ferraiuolo, Rosa Maria; Fifield, Bre Anne; Lubanska, Dorota; Oh, So Won; Cheon, Gi Jeong; Kwak, Cheol; Jeong, Chang Wook; Kang, Keon Wook; Trant, John F.; Morrissey, Colm; Coleman, Ilsa M.; Wang, Yuzhuo; and Ahmadzadehfar, Hojjat. (2020). Differential expression of glucose transporters and hexokinases in prostate cancer with a neuroendocrine gene signature: A mechanistic perspective for 18 F-FDG imaging of PSMA-suppressed tumors. *Journal of Nuclear Medicine*, 61 (6), 904-910.
https://scholar.uwindsor.ca/chemistrybiochemistrypub/184

Authors

Martin K. Bakht, Jessica M. Lovnicki, Janice Tubman, Keith F. Stringer, Jonathan Chiaramonte, Michael R. Reynolds, Iulian Derecichei, Rosa Maria Ferraiuolo, Bre Anne Fifield, Dorota Lubanska, So Won Oh, Gi Jeong Cheon, Cheol Kwak, Chang Wook Jeong, Keon Wook Kang, John F. Trant, Colm Morrissey, Ilsa M. Coleman, Yuzhuo Wang, and Hojjat Ahmadzadehfar

Differential expression of glucose transporters and hexokinases in prostate cancer with a neuroendocrine gene signature: a mechanistic perspective for FDG imaging of PSMA-suppressed tumors

Martin K. Bakht[1,2,3], Jessica M. Lovnicki[4], Janice Tubman[1], Keith F. Stringer[1,5], Jonathan Chiaramonte[6], Michael R. Reynolds[6], Iulian Derecichei[1], Rosa-Maria Ferraiuolo[7], Bre-Anne Fifield[1], Dorota Lubanska[1], So Won Oh[2,3], Gi Jeong Cheon[2,3*], Cheol Kwak[8], Chang Wook Jeong[8], Keon Wook Kang[2,3], John F. Trant[6], Colm Morrissey[9], Ilsa M. Coleman[10], Yuzhuo Wang[4], Hojjat Ahmadzadehfar[11], Xuesen Dong[4], Lisa A. Porter[1*]

[1]*Department of Biomedical Sciences, University of Windsor, Windsor, Ontario, Canada*

[2]*Department of Nuclear Medicine, Seoul National University College of Medicine, Seoul, Korea*

[3]*Laboratory of Molecular Imaging and Therapy, Cancer Research Institute, Seoul National University College of Medicine, Seoul, Korea*

[4]*Vancouver Prostate Centre, Department of Urologic Sciences, University of British Columbia, Vancouver, BC, Canada*

[5]*Department of Pathology, Cincinnati Children's Hospital Medical Center, Cincinnati, Ohio, USA*

[6]*Department of Chemistry and Biochemistry, University of Windsor, Windsor, Ontario, Canada*

[7]*Barbara Ann Karmanos Cancer Institute, Detroit, Michigan, USA.*

[8]*Department of Urology, Seoul National University College of Medicine, Seoul, Korea*

[9]*Department of Urology, University of Washington, Seattle, Washington, USA*

[10]*Divison of Human Biology, Fred Hutchinson Cancer Research Center, Seattle, Washington, USA*

[11]*Department of Nuclear Medicine, University Hospital Bonn, Bonn, 53127, Germany*

Word count: 4998

Running title: Glucose transport in neuroendocrine PC

Co-corresponding authors*:

***Gi Jeong Cheon,** *MD PhD*

Department of Nuclear Medicine, Seoul National University College of Medicine, Seoul 110-744, Korea

larrycheon@snu.ac.kr

***Lisa A. Porter,** *PhD*

Department of Biomedical Sciences, University of Windsor, Windsor, Ontario, N9B 3P4, Canada

lporter@uwindsor.ca

First author:

Martin K. Bakht, *PhD candidate*

Department of Biomedical Sciences, University of Windsor, Windsor, Ontario, Canada.

khosra11@uwindsor.ca

Financial support: This study was supported by Canadian Institutes of Health Research (#142189 (LAP) & #PJT156150 (XD)), Natural Sciences and Engineering Research Council of Canada #2018-06338 (JFT) and a grant of the Korea Health Technology R&D Project through the Korea Health Industry Development Institute, funded by the Ministry of Health & Welfare, Republic of Korea (#H18C1916 (GJC&KWK). The financial support of TELUS Ride for Dad, Prostate Cancer Fight Foundation (LAP) Banting Research Foundation (JFT) and Ontario Trillium Scholarship Program (MKB) is greatly appreciated. The gene expression analysis was supported in part by a Department of Defense Idea Development Award-Partnering-PI (W81XWH-17-1-0414;W81XWH-17-1-0415 (CM)) and the Pacific Northwest Prostate Cancer SPORE (P50CA97186 (CM)).

ABSTRACT

Purpose: Recent data suggests that low expression of prostate-specific membrane antigen (PSMA) is associated with a spectrum of neuroendocrine (NE) hallmarks and androgen receptor (AR)-suppression in prostate cancer (PC). Previous clinical reports indicate that PCs with a phenotype similar to NE tumors can be more amenable to imaging by ^{18}F-Fluorodeoxyglucose (FDG) rather than PSMA-targeting radioligands. In this study, we evaluated the association between NE gene signature and FDG uptake-associated genes including glucose transporters (GLUTs) and hexokinases, with the goal of providing a genomic signature to explain the reported FDG-avidity of PSMA-suppressed tumors.

Methods: Data mining approaches, cell lines and patient-derived xenograft (PDX) models were used to study the levels of 14 members of the *SLC2A* family (encoding GLUT proteins), 4 members of the hexokinase family (genes: *HK1* to *3* and *GCK*) and PSMA (*FOLH1* gene) following AR-inhibition and in correlation with NE hallmarks. Also, we characterize a NE-like PC (NELPC) subset among a cohort of primary and metastatic PC samples with no NE histopathology. We measured glucose uptake in a NE-induced *in vitro* model and a zebrafish model by non-radioactive imaging of glucose uptake using fluorescent glucose bioprobe, GB2-Cy3.

Results: This work demonstrates that a NE gene signature associates with differential expression of genes encoding GLUT and hexokinase proteins. In NELPC, elevated expression of *GCK* (encoding glucokinase protein) and decreased expression of *SLC2A12* correlated with earlier biochemical recurrence. In tumors treated with AR-inhibitors, high expression of *GCK* and low expression of *SLC2A12* correlated with NE histopathology and PSMA gene suppression. GLUT12-suppression and amplification of glucokinase was observed in NE-

induced PC cell lines and PDX models. A higher glucose uptake was confirmed in low-PSMA tumors using a GB2-Cy3 probe in a zebrafish model.

Conclusions: NE gene signature in NEPC and NELPC associates with a distinct transcriptional profile of GLUTs and HKs. PSMA-suppression correlates with GLUT12-supression and glucokinase-amplification. Alteration of FDG uptake-associated genes correlated positively with higher glucose uptake in AR and PSMA-suppressed tumors. Zebrafish xenograft tumor models are an accurate and efficient pre-clinical method for monitoring non-radioactive glucose uptake.

Key words: Neuroendocrine prostate cancer, PSMA, glucose transporters, hexokinases, glucokinase

INTRODUCTION

The androgen receptor (AR) plays a central role in regulating the transcriptional events driving prostate cancer (PC) progression and development of metastatic castration-resistant prostate cancer (mCRPC) (*1*). AR-inhibition is an effective therapeutic approach for most patients at different stages of PC. Although the incidence of *de novo* neuroendocrine (NE) PC (NEPC) is considered rare, several emerging forms of PC with low-levels of AR are identified. The suppression and low activity of AR in these patients is largely associated with a NE gene signature (NEGS) and resistance to AR-inhibition (*2*,*3*).

AR-directed therapy of mCRPC could promote cellular plasticity and development of an AR-suppressed phenotype similar to NEPC which manifests the histopathology of NE disease (*4*). Another emerging phenotype of mCRPC is AR-null and NE-null, classified as double-negative PC (DNPC) (*3*). A recent molecular subtyping of PC patients with no history of AR-directed therapies identified a NE-positive subtype with low chromatin binding and activity of AR. These patients have been referred to as NE-like PC (NELPC) since they do not represent the NE-histopathology (*2*,*5*). NEPC is associated with the loss of RE1-silencing transcription factor (REST) due to alternate splicing by the RNA splicing factor serine/arginine repetitive matrix 4 (*SRRM4*). *SRRM4* plays a crucial role in progression to NEPC under next-generation AR-inhibitors, such as abiraterone and enzalutamide (*6*). Hence, the elevation of *SRRM4* and the loss of its target *REST* could be specific markers of treatment-induced NEPC.

AR regulates the expression of *FOLH1* gene encoding the transmembrane protein, prostate-specific membrane antigen (PSMA). PSMA-targeted molecular imaging and therapy are transforming the landscape of PC management (*7*,*8*). Despite the impactful implications of PSMA, there are clinical reports that suggest that PSMA-targeted imaging does not effectively visualize NEPC tumors (*8-10*). Pre-clinical studies confirmed that the induction of lineage plasticity by AR-inhibition leads to NE-transdifferention and suppression of PSMA (*11*).

Similar to glucose, ^{18}F-fluorodeoxyglucose (FDG) is actively transported into the cell by the protein family of glucose transporters (GLUTs), encoded by *SLC2A* genes, followed by phosphorylation by hexokinase (*12*). In some types of tumors a positive correlation has been reported between FDG uptake and the levels of specific GLUTs and hexokinases (*12-14*). FDG-positron emission tomography (PET) is a well-accepted approach for delineation of proliferative and poorly-differentiated/dedifferentiated NE-tumors (*15*). Despite this, FDG-PET has been considered ineffective in assessing metastatic tumor burden and monitoring therapy response (*16*). Recent case reports illustrate NEPC delineation may be more feasible by FDG than PSMA-radioligands (*17,18*) and Spratt *et al*. (*19*) demonstrated the utility of FDG-PET for NEPC imaging. Interestingly, Thang *et al.* (*20*) screened patients with ^{68}Ga-PSMA-11 and FDG-PET and they identified a subset of patients with low PSMA-radioligand uptake and high FDG uptake.

Development of non-radioactive glucose analogs enabling the delineation of the glucose uptake of tumors have been studied using a variety of optical approaches mostly in mouse models (*21*). PC xenograft studies in zebrafish are coming to the forefront as a cost-effective and time-efficient model for drug screening, and the fluorescent glucose bioprobe GB2-Cy3 has been used to monitor glucose uptake in a zebrafish model (*22,23*). However, the feasibility of monitoring of glucose uptake in PC in a zebrafish model has not been evaluated.

In this work we used data mining approaches, cell lines and patient-derived xenograft (PDX) models to study expression levels of glucose uptake-associated genes including GLUTs and hexokinases in NEPC and NELPC to provide a genomic rationalization for the previously reported FDG-avidity of PSMA-suppressed PC tumors. We also present the feasibility of non-radioactive *in vivo* imaging of glucose uptake using a zebrafish model.

MATERIAL AND METHODS

Cell Culture

The LNCaP cell line was purchased from ATCC and grown in RPMI-1640 in the presence of 10% fetal bovine serum. Progression to NEPC was achieved by culturing LNCaP cells in RPMI1640 medium with 10% charcoal-stripped serum for 4 months. Under these conditions, cell morphology gradually changed into a mixture of a NE-like phenotype and a non-NE-phenotype. After 4 months, a subclone with a NE-like phenotype was isolated (LNCaP-NEPC). LNCaP cells, maintained in RPMI-1640 + fetal bovine serum, were used as a control and are referred to as LNCaP-AdPC.

Antibodies

The immunoblotting technique used was previously described (*11*). Antibodies are as follows: actin (Chemicon-Millipoure; MAB150-1R), PSMA (Cell Signaling; D4S1F), AR (Santa Cruz Biotechnology (SCB); sc-816), NSE (SCB; sc-271384) and GCK (SCB; sc-17819) and GLUT12 (Abcam; ab100993).

Data Mining Analysis

Using 268 PC samples from 3 different cohorts we assessed the transcript abundance for all of the *SLC2A* family (*SLC2A1-14*) and the HK family (*HK1-4*, *HK4* referred to as *GCK*). In addition, we monitored the PSMA gene (*FOLH1*), the NE-marker synaptophysin gene (*SYP*), *SRRM4* as a positive marker of treatment-induced NEPC and *REST* as negative marker of NEPC. Patients with lack of NEGS or NE histopathology are referred as adenocarcinoma PC (AdPC).

To assess the lineage plasticity of mCRPC, samples from a tissue acquisition necropsy platform established at the University of Washington (UW) were used (*3*). All rapid autopsy tissues were collected from patients who signed written informed consent under the aegis of the Prostate Cancer Donor Program at the UW and the Institutional Review Board of the UW approved this study. We classified our mCRPC subtypes as AdPC (AR^{+}/NE^{-}), AR-suppressed AdPC (AR^{low}/NE^{-}), NEPC (AR^{-}/NE^{+}), and DNPC (AR^{-}/NE^{-}). In addition, we used the Beltran

cohort (*4*) with histologically confirmed mCRPC-AdPC and mCRPC-NEPC samples. We identify a NELPC subset among AdPC tumors from the Memorial Sloan Kettering Cancer Center (MSKCC) cohort (*24*) using the meta-signature of prototypical high-grade NEPC (*25*). Gene set enrichment analysis (GSEA) was performed on the identified subsets using gene sets downloaded from the Molecular Signatures Database (*26*).

Mice PDX Models

Fresh PC tissues from patients were grafted under the kidney capsules of non-obese diabetic/severe combined immunodeficient mice. Institutional Review Board and Animal Care Committee of the University of British Columbia approved this study and all subjects signed a written informed consent. We previously characterized and validated these models (*27*).

GB2-Cy3 Synthesis and Cellular Uptake

Synthesis and *in vitro* uptake of a glucose bioprobe GB2-Cy3 was previously reported with some modifications (*22*,*28*,*29*). Full experimental details are provided in the Supplemental Material.

***In Vivo* Glucose Uptake Imaging**

Wild-type zebrafish (*Danio rerio*) were maintained following the Canadian Council on Animal Care Guidelines. *In vivo* uptake of GB2-Cy3 in was visualized in a zebrafish model by modifications of previous protocols (*23*,*30*). Full experimental details are provided in the Supplemental Material. This study was approved by the University of Windsor Animal Care Committee.

Statistical Analysis

Statistical analysis was done using GraphPad Prism (CA, USA). The results are expressed as the mean ± standard error of the mean (SEM). The box-whisker plots show the median (horizontal line), the interquartile range (margins of box) and the absolute range (vertical line). Differences between two groups were compared by unpaired Student's t-test. One-way

ANOVA followed by a Benjamini-Hochberg or Tukey adjustment. Neurite length was measured by manual tracing and determined using NIH ImageJ software as previously described (*11*,*31*). Pearson correlation was used for nearest neighbor analysis and pairwise-correlation of the studied genes. Kaplan-Meier plots and heatmaps were generated using camcAPP (*32*) and Broad Institute Morpheus software (MA, USA).

RESULTS

Differential Expression of *FOLH1, SLC2A* and *HK* in mCRPC

Figure 1A shows that expression of *SLC2A12* and *FOLH1* are the nearest neighbors to *AR* ($r > 0.6$, $P < 0.01$) and *GCK* is the furthest neighbour ($r = -0.6$, $P < 0.01$) in the UW cohort (*3*). We observed a significant suppression of *FOLH1* in low-AR mCRPC phenotypes including NEPC and DNPC samples (Fig. 1B). Figure 1C shows NEPC tumors have a 5-fold elevation of *GCK* ($P < 0.0001$) when compared to AR-positive samples. Alternatively, Fig. 1D demonstrates that NEPC and DNPC samples suppress expression of *SLC2A12*. Supplemental Figure 1 verifies that in the Beltran cohort (*4*) *FOLH1*-suppressed NEPC samples have similar profiles of glucose transporter gene expression. In summary, *GCK* gene expression is elevated and the *SLC2A12* gene is suppressed in NEPC.

Differential Expression of *SLC2A* and HK in NELPC

The meta-signature of prototypical high-grade NEPC (*25*) was employed to isolate a potential NELPC group among a population of metastatic and primary AdPC samples lacking NEPC histopathology (Supplemental Figs. 2 and 3). GSEA was done on the identified subset to confirm enrichment of NEGS (*26*). Figure 2A shows a lack of hallmarks of AR response in NELPC. Fig. 2B confirms the identified NELPC subset has NEGS proposed by Beltran *et al.* (*4*). The pie charts in Supplemental Figure 2 show that a NELPC hallmark can be observed in both primary and metastatic samples, with the more prevalent signature seen in metastatic samples. Supplemental Figure 4 shows that *SLC2A1, 3-5, 9, 10, 12-14* and *HK1, 2* genes cluster

with *REST*; herein referred to as *REST*-clustered genes. On the other hand, *SLC2A2, 6-8, 11, HK3* and *CGK* cluster with *SRRM4* and other NE-markers; herein referred to as *SRRM4*-clustered genes. Pairwise-correlation with *SRRM4* expression is presented in Supplemental Figures 5-7. Similar to NEPC, *SLC2A12* and *FOLH1* expression are decreased in NELPC relative to AdPC (Fig. 2C). *GCK* expression is significantly higher in NELPC.

The Association of *SLC2A* and *HK* with Gleason Score (GS) and Biochemical Recurrence in NELPC

Supplemental Figures 9-10 depict expression levels of the studied genes during progression of AdPC based on GS. The majority of *REST*-clustered *SLC2A* genes and *HKs* are either unchanged or suppressed at high GS while *SRRM4*-clustered genes are significantly increased in samples with high GS. Kaplan-Meier survival curves studying high and low expression levels of the studied genes are represented in Supplemental Figures 11-12. The high expression of *SRRM4*-clustered genes such as *GCK* and *REST*-clustered gene *SLC2A1* (as an exception) are significantly associated with decreased biochemical recurrence (log-rank *P*-value for *GCK*: 0.015). Interestingly, high levels of *REST*-clustered genes including *SLC2A12* are associated with shorter time to biochemical recurrence (log-rank *P*-value for *SLC2A12*: 0.012). Supplemental Table 1 summarises the performed analysis on NELPC.

***SLC2A12* Suppression and *GCK* Overexpression are Shared Among NEPC and NELPC**

RNA-seq data from 268 PC samples from the MSKCC (*24*), Beltran (*4*) and UW (*3*) cohorts were used to stratify *SLC2A1-14* and *HK1-4* genes into NE-clustered and AdPC-clustered groups (Supplemental Fig. 14). The intersection between the clustered genes in different cohorts and inclusion of the most differentially expressed genes showed that *GCK* is the most highly expressed gene and *SLC2A12* is the most suppressed gene in samples with a NEGS.

NEPC Has a Distinct *GCK*-Amplified and *SLC2A12*-Suppressed Signature in PDX Models

The LTL331 PDX is a model of PC progression from AdPC-to-NEPC. LTL331 tumors regress following castration, but relapse within 24 to 32 months with tumors harbouring NEPC phenotypes (*27*). Figure 3A demonstrates that *GCK* expression is minimal before progression to CRPC but reaches maximum levels following cellular plasticity to CRPC and NEPC. Conversely, *SLC2A12* expression is at its maximum level in hormone sensitive AdPC and, with a slight fluctuation, gradually levels decrease following castration. The expression of *SLC2A12* and *FOLH1* are the nearest neighbors to *AR* ($r > 0.6$, $P < 0.01$) and *GCK* is the furthest neighbour ($r = -0.87$, $P < 0.01$) in the UW cohort (*3*). Figure 3B shows in our other well characterized PDX models consisting of 20 AdPC and 3 NEPC models that we observe significant elevation of *GCK* and suppression of *SLC2A12* gene expression in the NEPC models. Overall, NEPC models have a *SLC2A12*-low and *GCK*-high signature.

Higher *In Vitro* and *In Vivo* Glucose Uptake in NE-induced Cell Lines

To investigate the role of progression to a NE phenotype on glucose uptake we used the well-characterized NE subclone cell line (LNCaP-NEPC) in which NEPC cells are derived from LNCaP cells (LNCaP-AdPC) by culturing in an androgen-depleted environment to mimic clinical androgen-deprivation therapy (*33*) (cartoon of process: Supplemental Fig. 15A; characterization of lines in Supplemental Fig. 15B-D). Figure 4A shows that protein levels of the NE marker NSE are increased in the LNCaP-NEPC, while PSMA and AR levels are significantly decreased. The LNCaP-NEPC cell line has a significantly higher level of glucokinase (GCK) protein and a significantly lower level of GLUT12 (Fig. 4B).

Supplemental Figures 16-23 demonstrate chemical characterisation of the GB2-Cy3. Supplemental Figure 24 illustrates GB2-Cy3 uptake and its localization in LNCaP cells. Figure 4C shows the LNCaP-NEPC cell line has a higher *in vitro* uptake of GB2-Cy3. Similarly, a zebrafish model was used for non-radioactive *in vivo* imaging of glucose uptake and displayed higher GB2-Cy3 in engrafted LNCaP-NEPC cells (Fig. 5). These observations indicate that

suppression of PSMA, AR and elevation of NE markers in LNCaP cell lines are associated with a differential level of glucose uptake, suppression of GLUT12 and elevation of glucokinase proteins.

DISCUSSION

The development of AR-indifferent and NE-positive tumor phenotypes through divergent clonal evolution as a mechanism of resistance to AR-inhibition in mCRPC is a well characterized concept (*3*,*4*). However, Stelloo *et al.* (*2*) identified a NELPC in a treatment naïve and primary cohort. Our work identified a NELPC subset among primary and metastatic samples with no history of exposure to next generation AR-inhibitors. Our data also shows that the incidence of NELPC is more prevalent in metastatic specimens. These data support that either AR-indifferent subsets of cells can exist among AdPC that possess a greater susceptibility for NE-transdifferentiation, or AR-indifferent, NE-like cells exist from an early time point and are gradually selected for during treatment pressures.

The isoforms of GLUTs are structurally and functionally related proteins with different affinities to glucose. They are expressed in different cells based on the metabolic necessity for glucose uptake (*34*). The elevation of glycolysis in NEPC has been previously reported (*35*,*36*). Irrespective of overall contribution of GLUT in glucose metabolism, GLUT and HK family members could be associated with FDG uptake (*13*,*14*). Like glucose, FDG is phosphorylated by HKs while their products, glucose-6-phosphate and FDG-6-phosphate, could have different levels of inhibition on HKs depending on their structure (*37*). Supplemental Figure 25 represents structural domains of the isoforms of human HK proteins (*38*). Glucokinase lacks the N-terminus domain and cannot be inhibited by either glucose-6-phosphate or FDG-6-phosphate.

GLUT11 is considered a high affinity glucose transporter and could be effectual in elevation of glucose uptake while it is amplified (*34*). McBrayer *et al.* (*39*) evaluated the

association of GLUT11 expression and FDG uptake in multiple myeloma. We have observed a significant elevation of GLUT11 expression in both NEPC and NELPC. Similarly, GLUT7 and 8 have high affinity to glucose (*40*) and we observe their amplification in samples with NEGS. Contrary to HK1-3, glucokinase which is known as a glucose sensor in pancreatic beta-cells, is not inhibited by its product glucose-6-phosphate but remains active while glucose is abundant (*37,38*). We can speculate that the apparent elevation of glucose uptake in NEPC or NELPC could be due to elevation of the expression of the aforementioned high affinity of GLUTs (Supplemental Fig. 26). While our study provides functional support for this conclusion, it is also important to remember the complications associated with a focus on gene expression of this vast family of glucose transport regulators. Avril's commentary (*13*) elaborates on the complex number of molecular, cellular, tissue and organ related variables regulating the resulting ^{18}F-FDG signal, all of which may provide inconsistencies between GLUT expression and the resulting ^{18}F-FDG signal.

GLUT1 is a high affinity and basal glucose transporter expressed ubiquitously in human tissues. In hormone sensitive PC, GLUT1 gene expression is positively correlated with androgen levels (*41*). Our work implies that GLUT1 expression has limited prognostic potential since it cannot estimate development or existence of low-AR phenotypes such as NEPC or DNPC phenotype. GLUT12 has been recently introduced as a downstream target of AR and its expression is tightly regulated by androgens (*42*). Our data demonstrated the *SLC2A12* suppression is also a highly associated with development of PSMA-low and NE-high gene signature in mCRPC. This work shows *GCK*-amplification and *SLC2A12* suppression correlate with the PSMA-suppression, higher GS and shorter time to biochemical recurrence in NELPC.

For pre-clinical studies, the use of FDG-imaging in mice xenografts can be limited by several factors such as operating cost and short half-life of the radioactive substance and

nonradioactive glucose probes, which are of particular interest (*21*). Also, the engraftment of tumors in mice can be challenging to establish and are time-consuming. This work demonstrates the feasibility of non-radioactive imaging of glucose uptake in PC xenografts using a zebrafish model as a rapid and cost-effective model.

Hope *et al.* (*7*) represented the detection rate of ^{68}Ga-PSMA-11 was estimated 0.94 for high- prostate-specific antigen (PSA) patients while this rate falls to 0.63 for low-PSA patients. Parida *at al.* (*18*) reported a NEPC patient with a low PSMA-radioligand uptake and a high FDG uptake. The identified low-PSA subclass of patients by Thang *et al.* (*20*) has similar imaging outcomes. The identification of this PSMA-low or discordant FDG-avid should be a high priory due to the apparent association with development of NEPC or DNPC.

CONCLUSION

NEPC, DNPC and NELPC have distinct differential expression of GLUT and HK genes. In accordance with this, the loss of PSMA in NEPC is associated with elevated glucose uptake.

DISCLOSURE

The authors declare no conflict of interest.

KEY POINTS

QUESTION: We investigated whether the expression levels of glucose uptake-associated genes are correlated with development of NEGS and/or suppression of the PSMA gene.

PERTINENT FINDINGS: Data mining approaches, cell lines, mouse and zebrafish PDX models were used to demonstrate that GLUT and HK expression, specially *GCK* and *SCL2A12*, are associated with NEGS, PSMA-suppression and higher glucose uptake.

IMPLICATIONS FOR PATIENT CARE: This study supports the use of FDG-PET for imaging of low-PSMA PC tumors with NEGS.

REFERENCES

1. Stelloo S, Bergman AM, Zwart W. Androgen receptor enhancer usage and the chromatin regulatory landscape in human prostate cancers. *Endocr Relat Cancer.* 2019;26.

2. Stelloo S, Nevedomskaya E, Kim Y, et al. Integrative epigenetic taxonomy of primary prostate cancer. *Nat Commun.* 2018;9:4900.

3. Bluemn EG, Coleman IM, Lucas JM, et al. Androgen receptor pathway-independent prostate cancer is sustained through FGF Signaling. *Cancer Cell.* 2017;32:474-489.e476.

4. Beltran H, Prandi D, Mosquera JM, et al. Divergent clonal evolution of castration resistant neuroendocrine prostate cancer. *Nat Med.* 2016;22:298-305.

5. Alshalalfa M, Liu Y, Wyatt AW, et al. Characterization of transcriptomic signature of primary prostate cancer analogous to prostatic small cell neuroendocrine carcinoma. *Int J Cancer.* 2019;in press.

6. Li Y, Donmez N, Sahinalp C, et al. SRRM4 drives neuroendocrine transdifferentiation of prostate adenocarcinoma under androgen receptor pathway inhibition. *Eur Urol* 2017;71:68-78.

7. Hope TA, Goodman JZ, Allen IE, Calais J, Fendler WP, Carroll PR. Meta-analysis of 68Ga-PSMA-11 PET accuracy for the detection of prostate cancer validated by histopathology. *J Nucl Med.* 2019;60:786-793.

8. Sheikhbahaei S, Afshar-Oromieh A, Eiber M, et al. Pearls and pitfalls in clinical interpretation of prostate-specific membrane antigen (PSMA)-targeted PET imaging. *Eur J Nucl Med Mol Imaging.* 2017;44:2117-2136.

9. Tosoian JJ, Gorin MA, Rowe SP, et al. Correlation of PSMA-targeted (18)F-DCFPyL PET/CT findings with immunohistochemical and genomic data in a patient with metastatic neuroendocrine prostate cancer. *Clin Genitourin Cancer.* 2017;15:e65-e68.

10. Chakraborty PS, Tripathi M, Agarwal KK, Kumar R, Vijay MK, Bal C. Metastatic poorly differentiated prostatic carcinoma with neuroendocrine differentiation: negative on 68Ga-PSMA PET/CT. *Clin Nucl Med.* 2015;40:e163-166.

11. Bakht MK, Derecichei I, Li Y, et al. Neuroendocrine differentiation of prostate cancer leads to PSMA suppression. *Endocr Relat Cancer.* 2019;26:131-146.

12. Haberkorn U, Ziegler SI, Oberdorfer F, et al. FDG uptake, tumor proliferation and expression of glycolysis associated genes in animal tumor models. *Nucl Med Biol* 1994;21:827-834.

13. Avril N. GLUT1 Expression in Tissue and 18F-FDG Uptake. *J Nucl Med.* 2004;45:930-932.

14. Yang H, Zhong JT, Zhou SH, Han HM. Roles of GLUT-1 and HK-II expression in the biological behavior of head and neck cancer. *Oncotarget.* 2019;10:3066-3083.

15. Bozkurt MF, Virgolini I, Balogova S, et al. Guideline for PET/CT imaging of neuroendocrine neoplasms with 68Ga-DOTA-conjugated somatostatin receptor targeting peptides and 18F–DOPA. *Eur J Nucl Med Mol Imaging.* 2017;44:1588-1601.

16. Jadvar H. PET of glucose metabolism and cellular proliferation in prostate cancer. *J Nucl Med.* 2016;57:25S.

17. Perez PM, Hope TA, Behr SC, van Zante A, Small EJ, Flavell RR. Intertumoral Heterogeneity of 18F-FDG and 68Ga-PSMA Uptake in Prostate Cancer Pulmonary Metastases. *Clin Nucl Med.* 2019;44:e28-e32.

18. Parida GK, Tripathy S, Datta Gupta S, et al. Adenocarcinoma Prostate With Neuroendocrine Differentiation: Potential Utility of 18F-FDG PET/CT and 68Ga-DOTANOC PET/CT Over 68Ga-PSMA PET/CT. *Clin Nucl Med.* 2018;43:248-249.

19. Spratt DE, Gavane S, Tarlinton L, et al. Utility of FDG-PET in clinical neuroendocrine prostate cancer. *Prostate.* 2014;74:1153-1159.

20. Thang SP, Violet J, Sandhu S, et al. Poor outcomes for patients with metastatic castration-resistant prostate cancer with low prostate-specific membrane antigen (PSMA) expression deemed ineligible for 177Lu-labelled PSMA radioligand therapy. *Eur Urol Oncol.* 2018;in press.

21. Cheng Z, Levi J, Xiong Z, et al. Near-infrared fluorescent deoxyglucose analogue for tumor optical imaging in cell culture and living mice. *Bioconjug Chem.* 2006;17:662-669.

22. Lee HY, Lee JJ, Park J, Park SB. Development of fluorescent glucose bioprobes and their application on real-time and quantitative monitoring of glucose uptake in living cells. *Chemistry.* 2011;17:143-150.

23. Melong N, Steele S, MacDonald M, et al. Enzalutamide inhibits testosterone-induced growth of human prostate cancer xenografts in zebrafish and can induce bradycardia. *Sci Rep.* 2017;7:14698.

24. Taylor BS, Schultz N, Hieronymus H, et al. Integrative genomic profiling of human prostate cancer. *Cancer Cell.* 2010;18:11-22.

25. Tsai HK, Lehrer J, Alshalalfa M, Erho N, Davicioni E, Lotan TL. Gene expression signatures of neuroendocrine prostate cancer and primary small cell prostatic carcinoma. *BMC Cancer.* 2017;17:759.

26. Subramanian A, Tamayo P, Mootha VK, et al. Gene set enrichment analysis: a knowledge-based approach for interpreting genome-wide expression profiles. *Proc Natl Acad Sci U S A* 2005;102:15545-15550.

27. Akamatsu S, Wyatt AW, Lin D, et al. The placental gene PEG10 promotes progression of neuroendocrine prostate cancer. *Cell Rep.* 2015;12:922-936.

28. Korbel GA, Lalic G, Shair MD. Reaction microarrays: a method for rapidly determining the enantiomeric excess of thousands of samples. *J Am Chem Soc.* 2001;123:361-362.

29. Park J, Lee HY, Cho MH, Park SB. Development of a cy3-labeled glucose bioprobe and its application in bioimaging and screening for anticancer agents. *Angew Chem Int Ed Engl.* 2007;46:2018-2022.

30. Park J, Um JI, Jo A, et al. Impact of molecular charge on GLUT-specific cellular uptake of glucose bioprobes and in vivo application of the glucose bioprobe, GB2-Cy3. *Chem Comm.* 2014;50:9251-9254.

31. Ding Y, Li Y, Lu L, et al. Inhibition of nischarin expression promotes Neurite outgrowth through regulation of PAK activity. *PLOS ONE.* 2015;10:e0144948.

32. Dunning MJ, Vowler SL, Lalonde E, et al. Mining human prostate cancer datasets: The "camcAPP" Shiny App. *EBioMedicine.* 2017;17:5-6.

33. Yuan T-C, Veeramani S, Lin F-F, et al. Androgen deprivation induces human prostate epithelial neuroendocrine differentiation of androgen-sensitive LNCaP cells. *Endocr Relat Cancer.* 2006;13:151-167.

34. Qian Y, Wang X, Chen X. Inhibitors of glucose transport and glycolysis as novel anticancer therapeutics. *World J Transl Med.* 2014;3:37-57.

35. Choi SYC, Ettinger SL, Lin D, et al. Targeting MCT 4 to reduce lactic acid secretion and glycolysis for treatment of neuroendocrine prostate cancer. *Cancer Med.* 2018.

36. Li W, Cohen A, Sun Y, et al. The role of CD44 in glucose metabolism in prostatic small cell neuroendocrine carcinoma. *Mol Cancer Res.* 2016;14:344-353.

37. McKerrecher D, Waring MJ. Chapter One - Property-Based Design in the Optimisation of Benzamide Glucokinase Activators: From Hit to Clinic. In: Lawton G, Witty DR, eds. *Prog Med Chem.* Vol 52: Elsevier; 2013:1-43.

38. Roberts DJ, Miyamoto S. Hexokinase II integrates energy metabolism and cellular protection: Akting on mitochondria and TORCing to autophagy. *Cell Death Differ.* 2015;22:364.

39. McBrayer SK, Cheng JC, Singhal S, Krett NL, Rosen ST, Shanmugam M. Multiple myeloma exhibits novel dependence on GLUT4, GLUT8, and GLUT11: implications for glucose transporter-directed therapy. *Blood.* 2012;119:4686-4697.

40. Gonzalez-Menendez P, Hevia D, Mayo JC, Sainz RM. The dark side of glucose transporters in prostate cancer: Are they a new feature to characterize carcinomas? *Int J Cancer.* 2018;142:2414-2424.

41. Vaz CV, Marques R, Alves MG, et al. Androgens enhance the glycolytic metabolism and lactate export in prostate cancer cells by modulating the expression of GLUT1, GLUT3, PFK, LDH and MCT4 genes. *J Cancer Res Clin Oncol.* 2016;142:5-16.

42. White MA, Tsouko E, Lin C, et al. GLUT12 promotes prostate cancer cell growth and is regulated by androgens and CaMKK2 signaling. *Endocr Relat Cancer.* 2018;25:453-469.

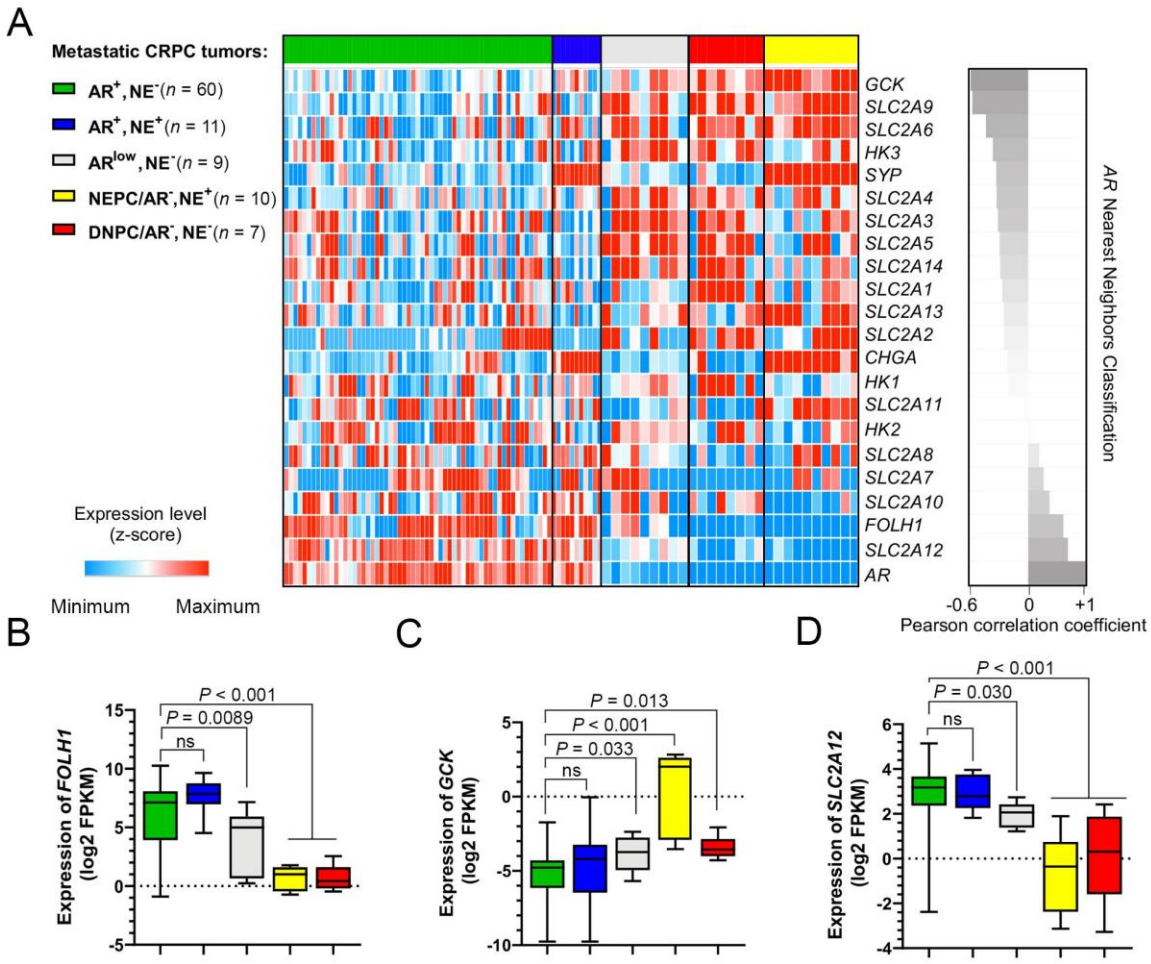

FIGURE 1. AR-negative subsets of mCRPC in UW cohort (*3*) have suppressed expression of *FOLH1* and differential expression of *SLC2A* and *HKs* genes. (A) The heatmap plot of the expression levels of *SLC2A* family members, *HK* genes, *AR*, *FOLH1* and NE-markers sorted based on nearest neighbors clustering to *AR*. (B-D) The box-whisker plots show the expression of *FOLH1*, *SLC2A12* and *GCK*.

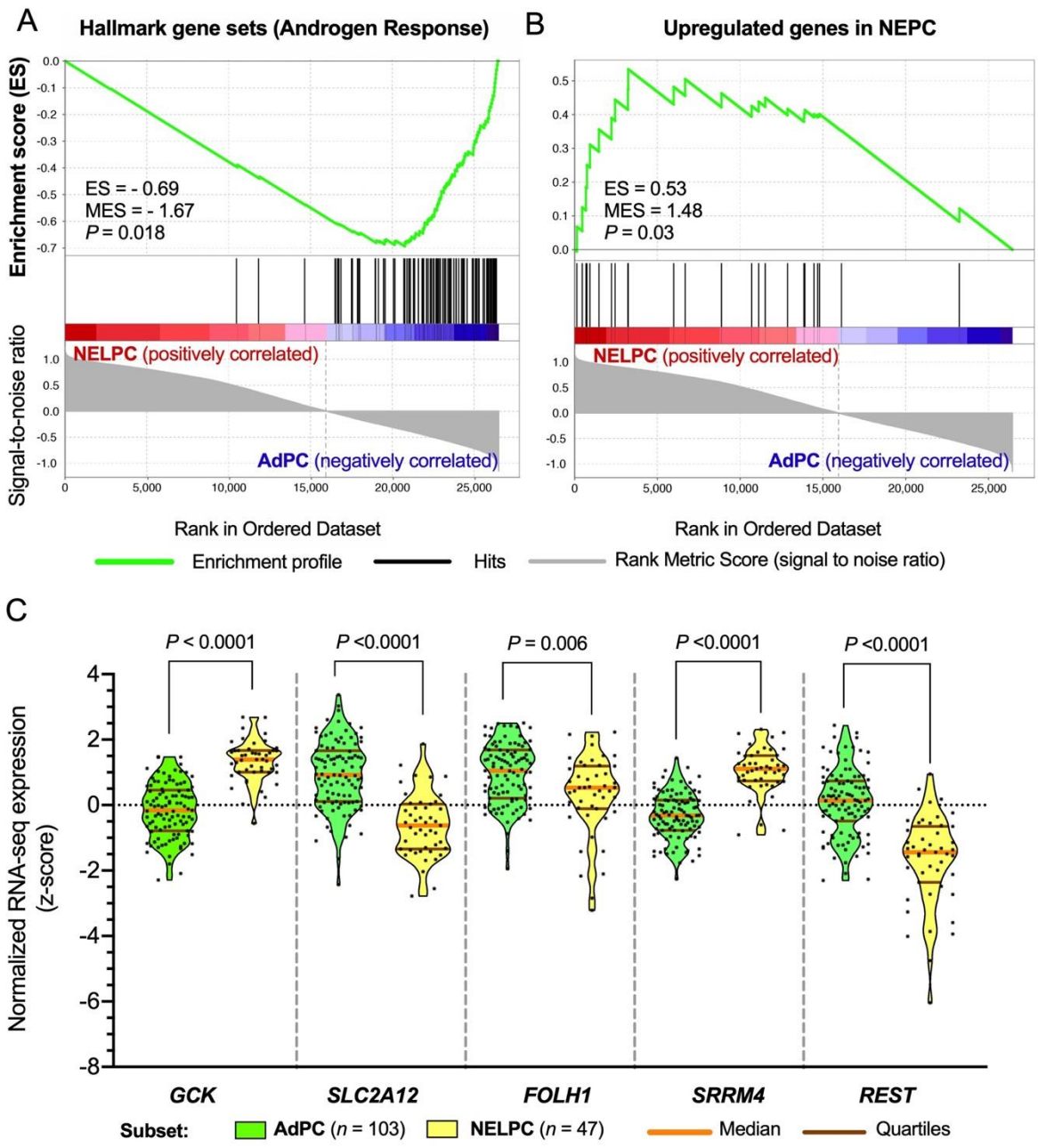

FIGURE 2. The NELPC subset of MSKCC cohort (*24*) displays (A) lack of AR response and (B) upregulation of NEPC makers recommended by Beltran *et al.* (*4*). (C) Violin plots compare the distribution of *SLC2A12*, *GCK* and *FOLH1*expressions in NELPC and AdPC subsets. NSE = Normalized enrichment score.

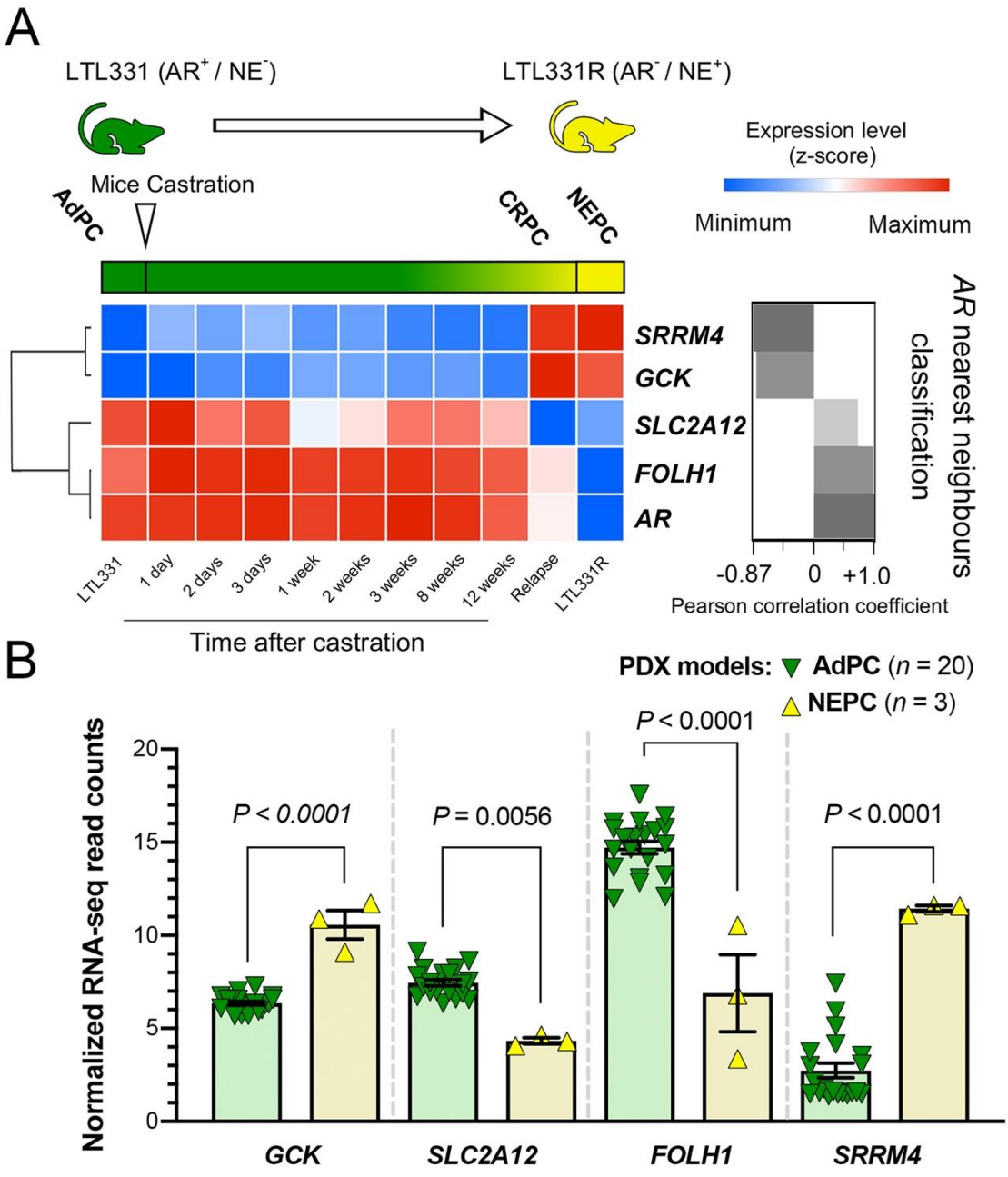

FIGURE 3. NEPC PDX models have suppressed expression of *FOLH1* and differential expressions of *SLC2A12* and *GCK*. (A) Transcription of the studied genes during progression to NEPC and correlation with *AR*. (B) The expression of the studied genes in PDX models.

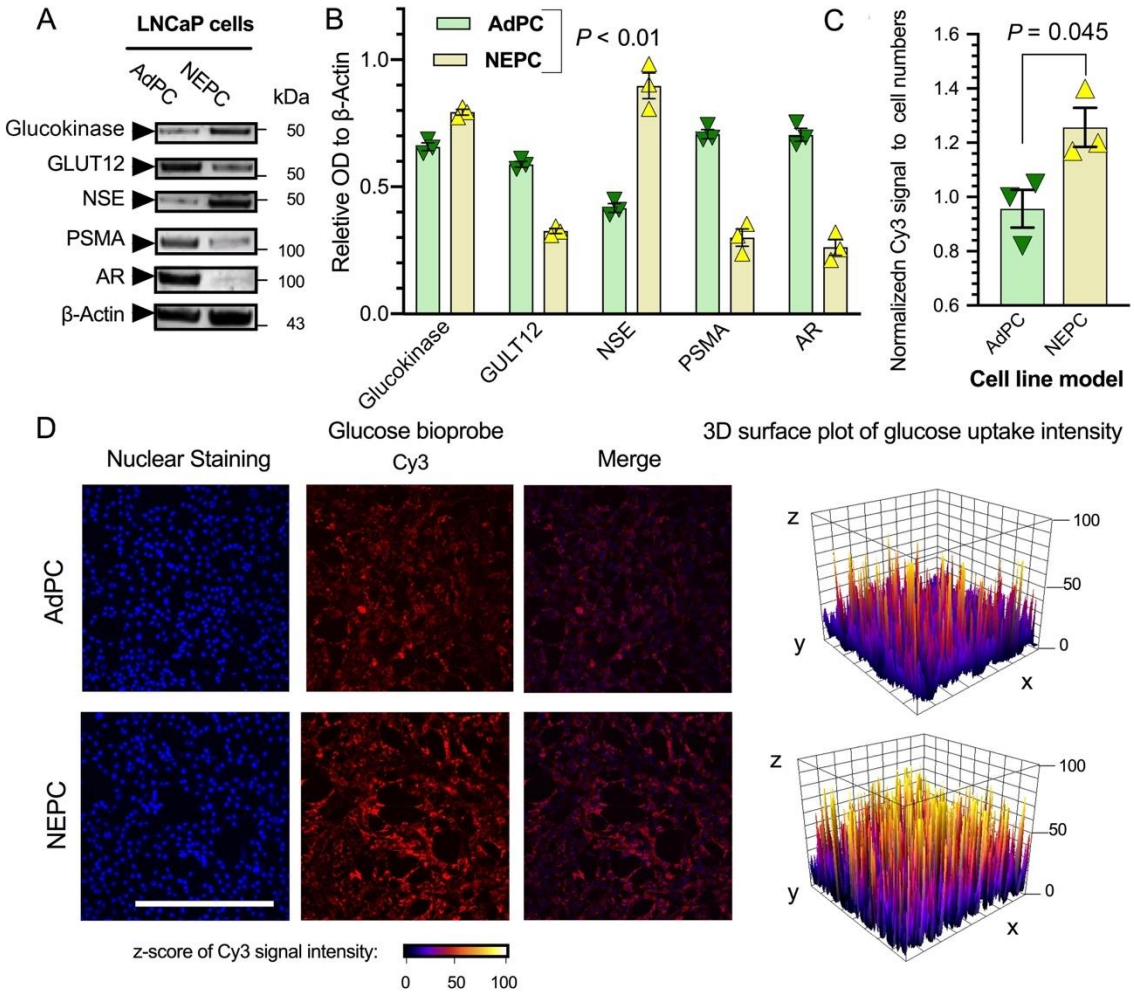

FIGURE 4. The NE-induced LNCaP cell line represents higher glucose uptake and differential protein levels of glucokinase and GLUT12. (A-B) Western blot analyses of protein levels. (C-D) Quantification of GB2-Cy3 uptake and representative images of LNCaP cells. Scale bar = 200 microns.

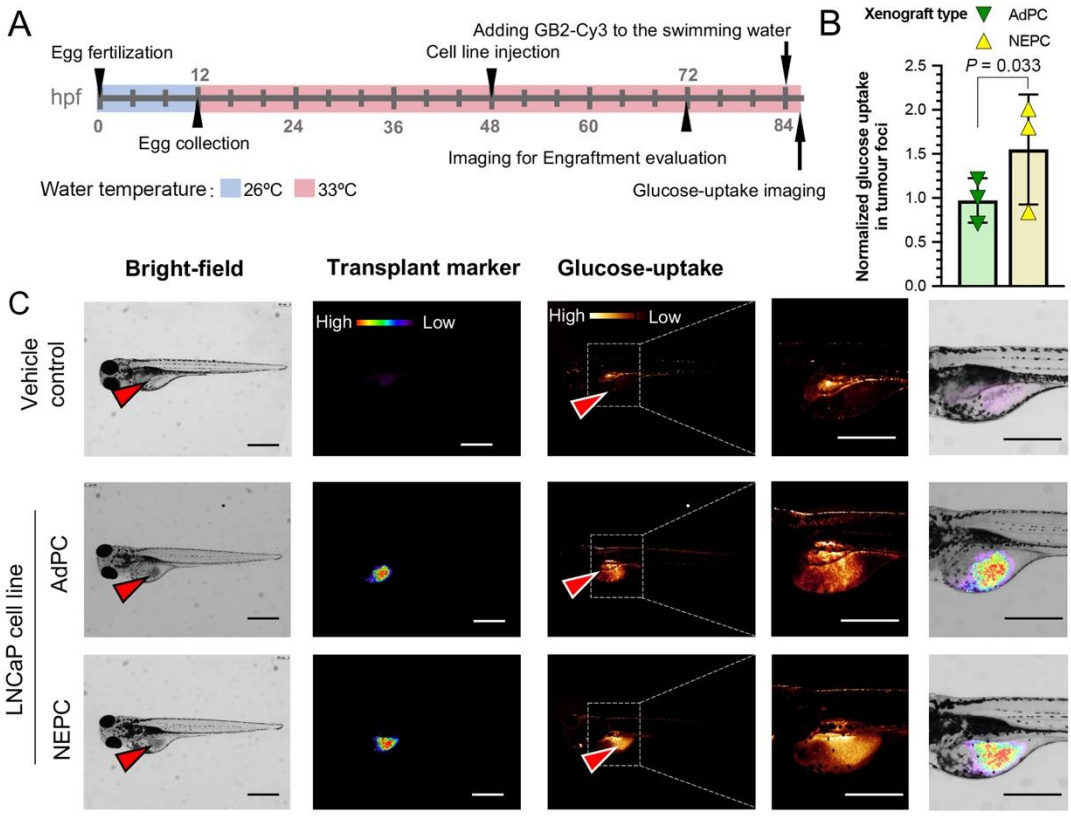

FIGURE 5. The NE-induced LNCaP cell line xenografts represent higher glucose uptake in a zebrafish model. (A) Schematic of the experiment. (B-C) Quantification of GB2-Cy3 uptake and representative images of embryos injected with different LNCaP cells. Red arrows show the injection sites. Scale bar = 200 microns.